Bull Volcanol (1998) 60:89–97

ORIGINAL PAPER

R. J. Stevenson · N. S. Bagdassarov · D. B. Dingwell
C. Romano

The influence of trace amounts of water on the viscosity of rhyolites

Received: 7 July 1997 / Accepted: 6 April 1998

Abstract As a major volatile in volcanic systems, water has a significant influence on the rheological properties of silicic magmas. This is especially so at minor water contents relevant to the emplacement of silicic lavas. To investigate the influence of water on the viscosity of natural rhyolitic obsidians, a novel strategy has been adopted employing parallel-plate and micropenetration techniques. Viscosities have been determined on three types of material: (a) raw water-bearing obsidians; (b) remelted (1650 °C, 1 atm) degassed glasses of the obsidians; and (c) hydrothermally hydrated (1300 °C, 3 kbar) obsidians. Ten natural rhyolitic obsidians (peraluminous, calc-alkaline and peralkaline) were employed: seven originated from lava flows and contained <0.2 wt.% H_2O, two samples were F-rich from pyroclastic successions, and one was an obsidian cobble with 1.5 wt.% water also associated with pyroclastic units. Melt compositions and water contents were stable during viscometry. The measured decreases in activation energies of viscous flow and viscosity with small amounts of water are much greater than the Shaw calculation scheme predicts. In addition, a marked non-linear decrease in η exists with increasing water content. In contrast to the case for peralkaline rhyolites, 0.1–0.2 wt.% water decreases activation energies significantly (up to 30%) for calc-alkaline compositions. These results have important implications for the ease of near-surface degassing of silicic magmas during emplacement and permit the testing of calculational models for viscosity, largely based on synthetic systems.

Key words Rhyolite · Calc-alkaline · Peralkaline · Viscosity · Water · Activation energy

Editorial responsibility: M. Carroll

R. J. Stevenson† · D. B. Dingwell (✉)
Bayerisches Geoinstitut, Universität Bayreuth, D-95440 Bayreuth, Germany

N. S. Bagdassarov
Institut für Meteorologie und Geophysik, Universität Frankfurt, D-60323 Franfurt, Germany

C. Romano
Dipartimento di Scienze della Terra, Terza Universitá degli Studi di Roma, 3, Largo San Murialdo 1, Rome, Italy
e-mail: don.dingwell@uni-bayreuth.de

† deceased

Introduction

Rheological experiments on the effect of water on the viscosity of natural melts are rare. Two reasons include the difficulty of measurement, because of the high pressures needed to dissolve significant amounts of water and the likelihood of vesicularity occurring at high temperatures and changing the physicochemical properties of the melt. For melts with less than 3 wt.% water, the situation is alleviated by the practice of viscosity measurements at 1 atm just above the glass transition region, where the kinetics of exsolution are slow (Richet et al. 1996; Dingwell et al. 1996). Furthermore, existing calculation schemes, such as that of Shaw (1972) for estimating the viscosity of water-bearing melts, are not very accurate at low water contents. Dingwell et al. (1996) studied the effect of water on a four-component haplogranitic melt (HPG8) approximating a calc-alkaline rhyolite and found an extremely non-linear decrease in viscosity with up to 3 wt.% added water. Richet et al. (1996) noticed a similar trend for an andesitic melt. Both studies noted poor agreement between their experimental data and viscosity calculated using the method of Shaw (1972). Hess and Dingwell (1996) summarized the available information on the effect of water on calc-alkaline rhyolite viscosities and generated a new model for predicting the viscosities of hydrous calc-alkaline rhyolites. The question remains unanswered, however, as to how well this calculation scheme, generated using data from synthetic systems, can be applied to natural hydrous rhyolitic compositions.

Here for the first time, viscosity experiments have been specifically performed on natural samples of both peralkaline and calc-alkaline rhyolitic compositions to examine the effects of small amounts of water on the rheological properties of magmas. In the field, peralkaline and calc-alkaline rhyolitic lava flows show differences in their vesiculation profiles (cf. Manley and Fink 1987; Stevenson et al. 1993) that provide implications for the ease of degassing and eruptive styles. Viscosity experiments were performed at volcanically relevant temperatures, from eruptive conditions to temperatures near the glass transition region. Furthermore, samples were specifically selected from nature and were crystal- and bubble poor. The range of sample water contents (0–1.5 wt.% H_2O) spans near-surface magmatic conditions prior to eruption and post-eruptive cooling of silicic lavas (Westrich et al. 1988; Lowenstern and Mahood 1991; Taylor 1991). In addition, viscosity experiments were performed on samples annealed at 1650 °C to remove water, and two series of samples hydrated under pressure with ~0.5 and ~1.0 wt.% water. These results are used to test viscosity model predictions, which are largely based on synthetic systems, and to refine viscosity estimates for the modelling of near-surface volcanic processes.

Sample description

Natural samples

The ten rhyolites used in this study are from: Erevan Dry Fountain, Armenia (two samples); Little Glass Butte, USA; Ben Lomond dome, Taupo Volcanic Center, New Zealand; St. Helena (California, USA); Red Hills (New Mexico, USA); 8ka flow and "Devils Staircase," Mayor Island, New Zealand; Eburru, Masaii Gorge, Kenya; and Macusani, southeast Peru. Of these ten rhyolites, three are of peralkaline composition, one is peraluminous, and the remaining six are calc-alkaline. Of the calc-alkaline rhyolites, only the Red Hills sample (RH) is from a pyroclastic deposit; the remainder are from lava flows. Of the peralkaline samples, the Eburru sample (KE5) was collected from a welded fall unit.

All starting samples were fresh, unweathered, unaltered, and non-hydrated obsidians free of cracks and containing few or no microlites. Sample BL6 from the Ben Lomond lava flow is a black, aphyric, sparsely spherulitic obsidian with <0.2 vol.% crystal content collected from a fault-scarp section bisecting two of the flow lobes of the dome (ca. 100 ka age).

EDF-1 and EDF-2 from Erevan Dry Fountain, Armenia, from the same lava flow, are compostionally identical gray Fe-poor, microlite-free glasses with different water contents. The sample from Little Glass Butte (LGB) also contains no microlites but has a higher Fe-content than the Armenian samples. The obsidian from St. Helena (SH) contained <0.2 vol.% microlites and was sampled from the glassy carapace of a lava dome. The only water-rich natural glass is an obsidian cobble (RH) from a pyroclastic deposit. This sample contains a small proportion of bubbles (ca. 6 vol.%) with volumetrically minor bands of microlite (ca. 1 vol.%) and bubbles.

The peraluminous macusanite glass (MAC) is a non-(secondary-) hydrated gray-green stream pebble (sample JV2 of Pichavant et al. 1987) possibly associated with an ash-flow tuff of peraluminous crustal origin. The obsidian from the spatter-fed 8ka lava flow (sample 8 ka) is an Fe-rich, peralkaline greenish-black obsidian containing some microvesicles. The other Mayor Island sample (DS1) is from a 1-m-thick glassy band within the upper part of a lava flow that forms an eroded caldera-wall remnant and has a volumetrically minor microlite content (<0.2 vol.%). In contrast, sample KE5, from a welded fall unit, is the most strongly peralkaline sample and contains no vesicles, although it is derived from a welded glassy lens 1–2 m thick within the Eburru pumice.

Preparation of annealed and hydrated samples

In order to prepare an essentially dry rhyolitic melt, chips (ca. 5 mm size) of the natural rhyolites described previously were vesiculated at 1300 °C (for calc-alkaline samples) and 1100 °C (for peralkaline and peraluminous samples) for a few minutes followed by crushing to a fine-grained powder. The powder was then incrementally annealed in a Pt crucible for several hours at 1650 °C and at atmospheric pressure followed by cooling to room temperature over 24 h. The end products (denoted by the suffix -r) contained no crystals, no bubbles, and had water contents of 0.01–0.04 wt.%.

In the geologic record, the majority of obsidians have water contents less than 0.2 wt.%. Some juvenile clasts in pumice-lapilli sequences contain water contents of 0.8–2 wt.%, but they tend to be small fragments (<10 mm size) containing crystals and cracks (Dunbar and Kyle 1992) less suitable for viscosity experiments. As a result, due to the rarity of crystal-, bubble- and crack-free obsidians in the volcanologic record with water contents >0.2 wt.%, two samples, one calc-alkaline (BL6-r) and one peralkaline (8ka-r), were hydrated under pressure. Powdered material was added to a Pt capsule, the equivalent of 0.5 and 1.0 wt.% distilled water was incorporated, and then the capsule containing the powder and water was sealed by arc welding. Capsules were examined for possible leakage by testing for weight loss after drying in an oven at 150 °C for at least 1 h. Oven drying also ensured that the water (as vapor) was evenly distributed throughout the interior of the capsule. The hydrated melt was synthesized in an internally heated pressure vessel (CRSCM-CRNS, Orleans, France) at 1300 °C in excess of 3 kbar pressure for 96 h (for ~1.0 wt.% added water) and 66 h for ~0.5 wt.% added water (cf. Roux et al. 1994). The end product

was a bubble-free glass of $35 \times 3.5 \times 5$ mm approximate size, suitable for micropenetration viscosity experiments described below.

Viscometry

Viscosity determinations on natural and annealed (remelted) pairs were performed in a vertical push-rod dilatometer using both the parallel-plate and micropenetration methods. For parallel-plate measurements, cylindrical samples (8×10 mm size) were drilled from hand specimens, and cylinder ends were ground flat and parallel. Experimental samples were heated to the temperature of interest at a rate of 10 °C/min, then deformed by up to 10% of its initial length between two parallel plates of alumina. These experiments were performed on natural calc-alkaline rhyolitic obsidians containing 0.1–0.4 wt.% water, at volcanologically relevant temperatures (780–930 °C), strain rates (10^{-5} to 10^{-7} s^{-1}), and stresses (10^3–10^5 Pa). For incompressible samples, which effectively adhere to the plates (the no-slip condition described by Fontana 1970), the following equation is used for calculating viscosity η_s:

$$\eta_s = \frac{2\pi M g h^5}{3V \cdot (2\pi h^3 + V)} \quad (1)$$

which is valid for a wide range of radius-thickness combinations (Gent 1960). M is the applied load, g = gravitational acceleration, V = sample volume, h = sample height, and $\cdot$ is strain rate (s^{-1}). Previous measurements of shear viscosity on NBS 711 standard melt and comparison with tabulated data (e.g., Bagdassarov and Dingwell 1992), as well as parallel-plate viscometry on a remelted or anhydrous rhyolite annealed at 1650 °C, have shown that η_s is reproducible to within ± 0.07 $\log_{10}$ units. For the experimental stresses and strain rates described previously, the rates of deformation are at least three orders of magnitude slower than those at which non-Newtonian deformation is expected to occur for these melts (Webb and Dingwell 1990) and no strain-rate or stress-dependent rheology was observed.

Parallel-plate viscometry of natural melts is possible within the viscosity range of 10^8–10^{11} Pa s. Over most of this experimental range, significant crystal growth/dissolution and bubble growth does not occur during the timescale of these experiments. When natural obsidians containing between 0.1 and 0.2 wt.% water, originating from near-surface levels, are heated at 1 atm to temperatures >100 °C above the glass transition, vesiculation can occur. Preliminary experiments were required to determine the "operating temperature window" for viscosity determinations between the lower temperature limit, resulting from relaxation problems at viscosities higher than 10^{11} Pa s, and the higher temperature limit at which melt vesiculation occurs within experimental timescales. An operating window is defined as that temperature range above the glass transition region in which no measureable drift in sample chemistry and texture occurs on the timescale of the experiment (Stevenson et al. 1995).

Once an operating window was established for each sample, the natural samples were heated to the required temperature at a constant rate (10 °C/min) and then held at a constant temperature as a series of loads was applied following the loading and unloading procedure previously described in Bagdassarov and Dingwell (1992). For each applied load, the change in length of the sample cylinder was measured every 30 s for periods of 15–30 min allowing the samples to adequately relax (Dingwell and Webb 1990).

Micropenetration viscosity measurements were performed on the hydrated samples by indenting the surface of the melt at high viscosities. The indentor is an alumina sphere with a diameter of 3 mm nested in the lower end of a hollow silica push rod. Viscosity was determined using the following expression:

$$\eta = \frac{0.1875 M g t}{R^{0.5} \alpha^{0.5}} \quad (2)$$

where M is the applied load (kg), t is time (s), g is the acceleration due to gravity, R is radius of the indenter (m), and α is the micropenetration depth (m) (Pocklington 1940, Tobolsky and Taylor 1962). Because only a small amount of sample was available, the micropenetration method was used rather than the parallel-plate method, on doubly polished slices of 1.5–2 mm thickness. The samples were indented by no more than 5% of the total sample thickness.

Analysis of water contents

To test for any compositional drift in the samples during the course of experiments, chemical analyses were determined on both pre- and post-viscometry samples using ICP-AES and electron probe. Water contents were determined using a Bruker IFS 120HR Fourier Transform Spectometer to obtain transmission infrared spectra in the near-infrared region (2500–8000 cm^{-1}) using a W-source, CaF_2 beam-splitter, and a narrow-band MCT detector. The spectrophotometer operated at a resolution of 4 cm^{-1} with a scanning speed of 20 KHz. Typically, 200–500 scans were collected for each spectrum using an IR microscope equipped with a Cassegrain 15× objective. The background was recorded and subtracted from every spectrum. Unmounted doubly polished glass disks of ~0.5–2 mm thickness were analyzed. Integrated molar absorptivities of 248 ± 24 and 341 ± 25 l/mol cm^2 were used for the 5200 cm^{-1} (molecular H_2O) and 4500 cm^{-1} (OH^-) near-infrared peaks, respectively, and an integrated absorptivity of 44000 l/mol cm^2 was used for the 3750 cm^{-1} peak (molecular H_2O and OH^-; Newman et al. 1986). The precision of these measurements is based

on the reproducibility of the spectra obtained from duplicate analyses on the same spot, as well as uncertainty assigned to the background subtraction procedure. We estimate that the typical uncertainty in our measurements for these absorption bands is 2% relative. The concentration of dissolved total water in our samples was determined using the equation described by Stolper (1982).

Results

Composition and water contents

Chemical compositions and water contents determined by FTIR are listed in Table 1. ICP-AES and electron probe data (normalized to volatile-free conditions) show that the major element oxide compositons of the natural obsidian and anhydrous (or remelted) equivalents are the same. The only difference is in volatile content, which consists largely of water. For F-rich peralkaline and peraluminous samples, however, some F loss occurs on annealing at 1650 °C, as indicated by ion-specific electrode measurements. For Fe-rich peralkaline rhyolites, the Fe^{3+}/Fe_{total} ratio remains constant during viscometry experiments (Stevenson et al. 1995). However, when synthesizing an equivalent remelted sample, the Fe^{3+}/Fe_{total} increases from 0.30 for the natural starting material to 0.53. Experiments on more Fe-rich melts by Dingwell (1991) have shown that changes of this magnitude in Fe^{3+} content do not significantly affect the viscosity of Fe-bearing melts. Although those measurements were at higher temperatures than the experiments of the present study, the lower concentrations of Fe in the present samples will diminish the significance of any redox effects. Also, for Fe-rich peralkaline rhyolites we did not observe an order of magnitude increase with viscosity over time as did Neuville et al. (1993) for an andesitic melt. Unlike the experiments by Neuville et al. (1993), which were performed over a 116-h period, our viscometry experiments occurred within a short time interval of <7 h. Our samples were appropriately relaxed and compositionally unchanged, as demonstrated by stable and constant viscometry readings and postviscometry analysis, respectively.

Water contents were monitored before and after viscometry experiments by FTIR and showed no significant change (Table 2). Several measurements performed along traverses across sample disks (especially from the hydrated samples and the RH sample) showed no evidence for heterogeneity. Also, no loss of water occurred during viscometry experiments. For these samples, the water occurs mostly as OH^-. However, for natural water-poor obsidians and their annealed equivalents, the total water content is assumed to be entirely OH^-. At 1 atm pressure and 1650 °C, the equilibrium water content in remelted samples is no more than a few hundred parts per million. Some peralkaline rhyolite samples showed increased spectral noise above 6000 cm^{-1} due to a high Fe-content and an optical opacity. This effect was absent for Fe-poor calc-alkaline rhyolites. Nevertheless, this problem did not significantly affect the precision of measurements.

Viscosity

Viscometry results on all samples are listed in Table 3. Over the viscosity range 10^8–10^{12} Pa s, the $\log_{10}$ viscosity-inverse temperature relationship for these melts is Arrhenian with the following form:

$$\log_{10}\eta_s = \log_{10}A_\eta + \frac{E_\eta}{2.303\,R\,T} \quad (3)$$

where η_s is the viscosity at temperature T (K), and A_η and E_η are the pre-exponential factor and the activation energy of viscous flow, respectively, and R is the gas constant. Values for A_η and E_η are listed in Table 4.

Discussion

The effect on viscosity of the addition of small amounts of water is shown (see Fig. 1) for samples EDF-1 (0.06 wt.% water) and EDF-2 (0.13 wt.% water) from the same lava flow with EDF-r as a reference. Here, the small additions of water appear to progressively decrease the temperature dependence of viscosity (E_η decreases). At a constant temperature (e.g., $10^4/T = 10$), viscosity decreases by 1.3 $\log_{10}$ Pa s as water content increases from 0.06 to 0.13 wt.%. Both parallel-plate and

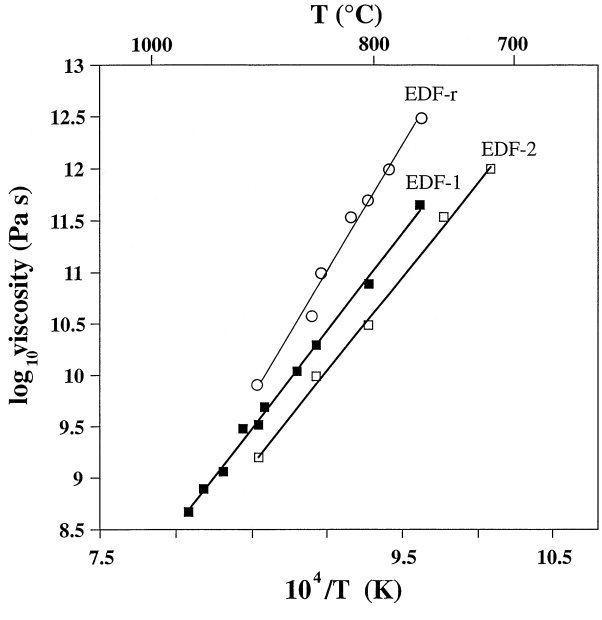

Fig. 1 Log viscosity vs inverse temperature for anhydrous EDF-r (*filled circles*); EDF-1 with 0.06 wt.% water (*filled squares*), and EDF-2 with 0.13 wt.% water (*open squares*)

Table 1 ICP AES and electron microprobe compositions of experimental samples

	BL6	BL6-r	SH	SH-r	LGB EMP ($n=11$)	LGB-r EMP ($n=11$)
SiO_2	77.48	77.53	77.17	77.08	76.92 (0.16)	77.88 (0.13)
TiO_2	0.17	0.17	0.08	0.09	0.10 (0.02)	0.07 (0.02)
Al_2O_3	12.20	12.17	12.40	12.44	12.92 (0.08)	12.73 (0.06)
FeO_t	1.30	1.30	1.30	1.30	0.89 (0.06)	0.76 (0.04)
MnO	0.05	0.05	0.02	0.02	0.05 (0.02)	0.04 (0.02)
MgO	0.17	0.17	0.01	0.02	0.11 (0.01)	0.06 (0.01)
CaO	1.14	1.13	0.35	0.36	0.86 (0.03)	0.50 (0.03)
Na_2O	3.90	3.89	4.5	4.49	3.89 (0.05)	3.93 (0.07)
K_2O	3.60	3.60	4.2	4.2	4.25 (0.06)	4.03 (0.04)
P_2O_5	< dtl	< dtl	< dtl	< dtl	0.03 (0.02)	0.01 (0.02)
Total	100.03	100.22	98.35	98.08	99.40	97.91
H_2O	0.13	0.04	0.12	0.04	0.08	0.02
AI	0.85	0.85	0.96	0.96	0.85	0.85

Table 1 (continued)

	RH	RH-r	MAC EMP ($n=20$)	MAC-r	EDF-1	EDF-2
SiO_2	76.99	77.01	74.39 (0.13)	74.04	78.00	78.00
TiO_2	0.03	0.03	0.05 (0.02)	0.03	0.09	0.09
Al_2O_3	13.02	13.14	16.13 (0.09)	16.22	12.15	12.15
FeO_t	0.71	0.71	0.59 (0.05)	0.50	0.54	0.54
MnO	0.10	0.10	0.08 (0.04)	0.01	0.07	0.07
MgO	0.04	0.04	0.02 (0.01)	0.03	0.06	0.07
CaO	0.48	0.51	0.22 (0.01)	0.19	0.50	0.50
Na_2O	4.31	4.28	4.24 (0.06)	4.16	4.08	4.08
K_2O	4.31	4.18	3.71 (0.05)	3.63	4.48	4.48
P_2O_5	< dtl	< dtl	0.58 (0.05)	n.d.	0.02	< dtl
Total	97.54	98.17	97.48 (0.47)	97.98	100.38	100.38
H_2O	1.49	0.01	0.16	0.02	0.06	0.13
F	–	–	1.34	1.05		
AI	0.90	0.88	0.68	0.66	0.95	0.95

Table 1 (continued)

	8ka	8ka-r	8ka-H (1.0) EMP ($n=20$)	DS1	DS1-r EMP ($n=14$)	KE5	KE5-r EMP ($n=14$)
SiO_2	73.78	73.94	74.55 (0.45)	75.30	75.69 (0.14)	72.50	73.15 (0.15)
TiO_2	0.22	0.22	0.23 (0.02)	0.24	0.23 (0.02)	0.28	0.29 (0.03)
Al_2O_3	9.64	9.68	9.66 (0.10)	10.0	9.66 (0.01)	8.10	8.32 (0.08)
FeO_t	5.82	5.79	5.08 (0.32)	4.40	5.08 (0.06)	7.70	7.10 (0.12)
MnO	0.13	0.13	0.13 (0.03)	0.09	0.13 (0.03)	0.21	0.22 (0.03)
MgO	0.02	0.02	0.03 (0.01)	< dtl	0.01 (0.01)	0.01	0.01 (0.01)
CaO	0.25	0.25	0.22 (0.02)	0.16	0.23 (0.02)	0.24	0.27 (0.02)
Na_2O	6.02	5.99	5.81 (0.13)	5.50	5.00 (0.05)	6.70	6.36 (0.05)
K_2O	4.12	3.99	4.28 (0.09)	4.20	4.30 (0.05)	4.30	4.27 (0.06)
P_2O_5	< dtl	< dtl	0.01 (0.01)	< dtl	0.02 (0.02)	< dtl	0.01 (0.02)
Total	99.62	100.22	96.36 (1.04)	90.69	98.72 (0.39)	99.04	97.53 (0.38)
H_2O	0.12	0.03	0.78	0.13	0.03	0.14	0.02
F	0.05	0.04		0.05	0.04	0.41	0.26
Fe^{3+}/Fe_t	0.33	0.53					
AI	1.49	1.46	1.47	1.36	1.25	1.94	1.81

Electron microprobe (EMP) analyses of glasses are listed as mean ±1SD (in parentheses) of *n* points. Analytical conditions include an accelerating voltage of 15 kV (10 nA) and a defocussed beam to minimise volatilisation of Na. Peak count time was 20 s with a background of 10 s using mineral standards. All data were normalised to 100% volatile-free, and original analytical totals are given. AI = agpaitic index (mol Na + K/Al). < dtl = less than delection limit. FeOt = total Fe as FeO. F was determined by ion-specific electrode. For DS1-r and KE5-r analysed by EMP, ICP analyses (with the exception of Si) were performed. ICP analyses of all other major elements were the same for natural and re-melted pairs

Table 2 Water contents before and after viscometry for water-rich natural and experimentally hydrated samples

Sample	Conditions	T (°C)	H_2O (wt. %)	OH (wt. %)	H_2Ot (wt. %)
RH-n	Raw	–	0.80	0.70	1.50
	Post η	450	0.75	0.76	1.51
		485	0.69	0.77	1.46
		501	0.68	0.78	1.46
		521	0.60	0.77	1.37
		549	0.66	0.79	1.44
		569	0.57	0.77	1.34
		589	0.55	0.75	1.29
BL6H0.5	Raw	–	0.07	0.41	0.48 (0.02)
BL6H1.0	Raw	–	0.27	0.68	0.96 (0.05)
	Post η	600	0.35	0.66	1.02
	Post η	649	0.34	0.66	1.00
8kaH0.4	Raw	–	0.08	0.29	0.37 (0.03)
8kaH0.8	raw	–	0.23	0.56	0.79 (0.02)
	Post η	500	0.32	0.53	0.85
	Post η	550	0.27	0.53	0.80

micropenetration measurements were perfomed on EDF-1 and show that both methods give consistent results (see Table 3). Also, because both natural samples came from the same lava flow, EDF-1 and EDF-2 are identical in major element oxide composition. The only significant compositional variable in this case is water.

The addition (or loss) of larger amounts of water (e.g., ~1.5 wt.%) profoundly affects viscosity, as shown in Fig. 2 for the Red Hills sample. For a constant T (e.g., $10^4/T = 10$) the effect of 1.5 wt.% water decreases viscosity by five to six orders of magnitude. Because water depresses η significantly, experiments on the natural sample could only be performed close to the glass transition region at temperatures below those considered magmatically relevant for rhyolitic magmas (e.g., 750–850 °C; Ghiorso and Sack 1991). At higher temperatures (T>550 °C), some microvesiculation occurred,

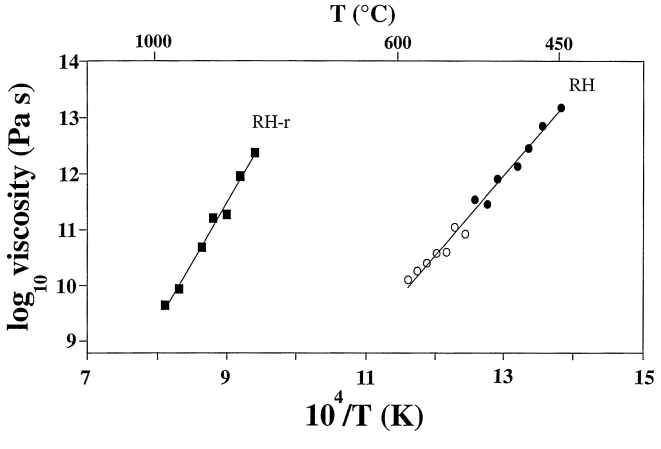

Fig. 2 Log viscosity vs inverse temperature for RH-r (*squares*) and RH with 1.5 wt.% water (*filled circles*) through which the regression line has been fitted. The addition or loss of 1.5 wt.% water causes a pronounced shift in T and η. For those samples >520 °C (*open circles*), some minor water losses occurred during experiment together with some microvesiculation at T>550 °C

Table 3 Viscosity data

	T (°C)	Log η (Pa s)		T (°C)	Log η Pa s)
BL6	915	8.50 (0.06)	EDF-2	751	11.54
(pp)	879	9.10 (0.07)	(mp)	719	12.00
	854	9.51 (0.04)			
	820	10.05 (0.04)	EDF-1	965	8.66 (0.04)
	820	10.25 (0.05)	(p/mp)	950	8.89 (0.05)
	788	10.62 (0.06)		931	9.06 (0.05)
				912	9.48 (0.03)
BL6-r	861	10.07 (0.02)		898	9.51
(pp)	879	9.81 (0.04)		892.5	9.69 (0.02)
	886	9.62 (0.04)		863.7	10.04 (0.05)
	905	9.34 (0.04)		846.7	10.29
	914	9.09 (0.03)		804.6	10.89
	923	9.04 (0.03)		767.1	11.65
	951.5	8.62 (0.02)			
			EDF-r	898	9.91
BL6H0.5	650	11.13 (0.01)	(mp)	851	10.58
(mp)	664	10.76 (0.005)		843	10.99
	678	10.51 (0.005)		820	11.54
	697	10.19 (0.001)		805	11.70
	717	9.77 (0.006)		790	11.99
				767	12.48
BL6H1.0	599	10.86 (0.01)			
(mp)	599.5	10.88 (0.01)	RH	450	13.18 (0.06)
	609	10.70 (0.01)	(mp)	464	12.85 (0.04)
	629	10.20 (0.01)		475	12.45 (0.05)
	640	9.88 (0.001)		485	12.14 (0.01)
				501	11.91 (0.02)
LGB	948	8.64 (0.04)		511	11.45 (0.03)
(pp)	933	8.81 (0.01)		521	11.55 (0.03)
	906	9.20 (0.08)		531	10.92 (0.03)
	878	9.65 (0.04)		541	11.05 (0.02)
	865	9.82 (0.05)		549	10.60 (0.02)
				559	10.58 (0.01)
LGB-r	912	10.12 (0.07)		569	10.39 (0.02)
(pp)	935	9.79 (0.07)		578	10.26 (0.02)
				589	10.10 (0.02)
SH	797	10.16 (0.04)			
(pp)	819	10.08 (0.01)	RH-r	960	9.64 (0.01)
	827	9.93 (0.0.5)	(mp)	932	9.93 (0.02)
	856	9.53 (0.04)		885	10.69 (0.03)
	885	8.96 (0.01)		862	11.20 (0.02)
	914	8.57 (0.02)		838	11.27 (0.03)
				815	11.95 (0.02)
SH-r	958	8.84 (0.02)		791	12.38 (0.11)
(pp)	933.5	9.16 (0.03)			
	906	9.51 (0.06)	MAC	812	8.25 (0.07)
	888	9.71 (0.05)	(pp)	791	8.63 (0.07)
	869	9.98 (0.05)		753	9.26 (0.06)
				737.5	9.37 (0.07)
EDF-2	898	9.20		713	9.72 (0.08)
(mp)	847	9.99		674	10.46 (0.12)
	805	10.49			
MAC-r	694	10.85	DS1	740	8.86 (0.02)
(mp)	723	10.37	(pp)	724	9.14 (0.03)
	763	9.85		715	9.29 (0.05)
	790	9.51		696	9.65 (0.02)
8ka	692	8.87 (0.04)		676	9.97 (0.05)
(pp)	683	9.14 (0.02)	DS1-r	696	10.40 (0.05)
	663	9.47 (0.02)	(pp)	730	9.68 (0.04)
	658	9.59 (0.05)		745	9.47 (0.03)
	645	9.81 (0.04)		769	9.16 (0.02)
	624	10.26 (0.02)		793	8.70 (0.03)
8ka-r	677	10.05 (0.06)	KE5	681.5	7.77 (0.06)
(pp)	696	9.71 (0.02)	(pp)	662	8.06 (0.07)
	715	9.32 (0.04)		648	8.29 (0.02)
	744	8.77 (0.03)		632	8.57 (0.02)
	769	8.43 (0.04)		612	8.92 (0.06)
	787	8.18 (0.09)		587	9.49 (0.02)
				568	9.97 (0.02)

Table 3 continued

	T (°C)	Log η (Pa s)		T (°C)	Log η Pa s)
8kaH0.4	551	11.00 (0.01)	KE5-r	657	9.18 (0.02)
(mp)	556	10.76 (0.01)	(mp)	667.5	8.95 (0.06)
	567	10.58 (0.005)		677	8.71 (0.02)
	586	10.17 (0.01)		696	8.42 (0.03)
	601	10.04 (0.003)		716	8.12 (0.06)
	621	9.55 (0.005)		716	8.15 (0.03)
8kaH0.8	500	11.04 (0.01)		764	7.42 (0.05)
(mp)	520	10.60 (0.005)			
	530	10.44 (0.005)			
	540	10.17 (0.001)			
	550	9.89 (0.005)			

pp = parallel-plate viscometry; mp = micropenetration viscometry
Numbers in parentheses refer to uncertainties based on the quality of the experimental deformation trace, where available

Table 4 Pre-exponential factor and activation energies of viscous flow determined for all viscometry samples

Sample	$Log_{10}A_\eta$	E_η (kJ/mol)
EDF-r	−10.903 (0.112)	466.17 (24.51)
EDF-1	− 6.645 (0.063)	363.26 (8.17)
EDF-2	− 6.365 (0.094)	348.98 (14.13)
BL6-r	− 9.927 (0.050)	434.05 (18.56)
BL6	− 8.709 (0.057)	392.18 (11.92)
BL6-H (0.5)	− 8.265 (0.047)	341.98 (15.53)
BL6-H (1.0)	− 8.019 (0.035)	315.52 (12.67)
LGB-r	− 9.018 (0.166)	435.09 (13.67)
LGB	− 7.920 (0.042)	386.69 (7.67)
SH-r	− 5.678 (0.021)	342.38 (7.95)
SH	− 7.053 (0.121)	356.19 (30.18)
RH-r	− 7.711 (0.121)	408.17 (20.20)
RH (T < 520 °C)	− 6.655 (0.126)	274.21 (22.18)
MAC-r	− 3.901 (0.031)	272.72 (8.23)
MAC	− 6.385 (0.073)	305.21 (13.36)
8ka-r	− 8.163 (0.042)	331.09 (8.35)
8ka	− 8.802 (0.039)	327.41 (11.54)
8ka-H (0.5)	− 6.327 (0.075)	272.11 (17.4)
8ka-H (1.0)	− 7.560 (0.051)	275.62 (16.0)
KE5-r	− 7.682 (0.041)	299.2 (8.44)
KE5	− 8.628 (0.053)	296.72 (7.65)
DS1-r	− 7.723 (0.060)	335.36 (16.05)
DS1	− 7.698 (0.019)	321.32 (6.90)

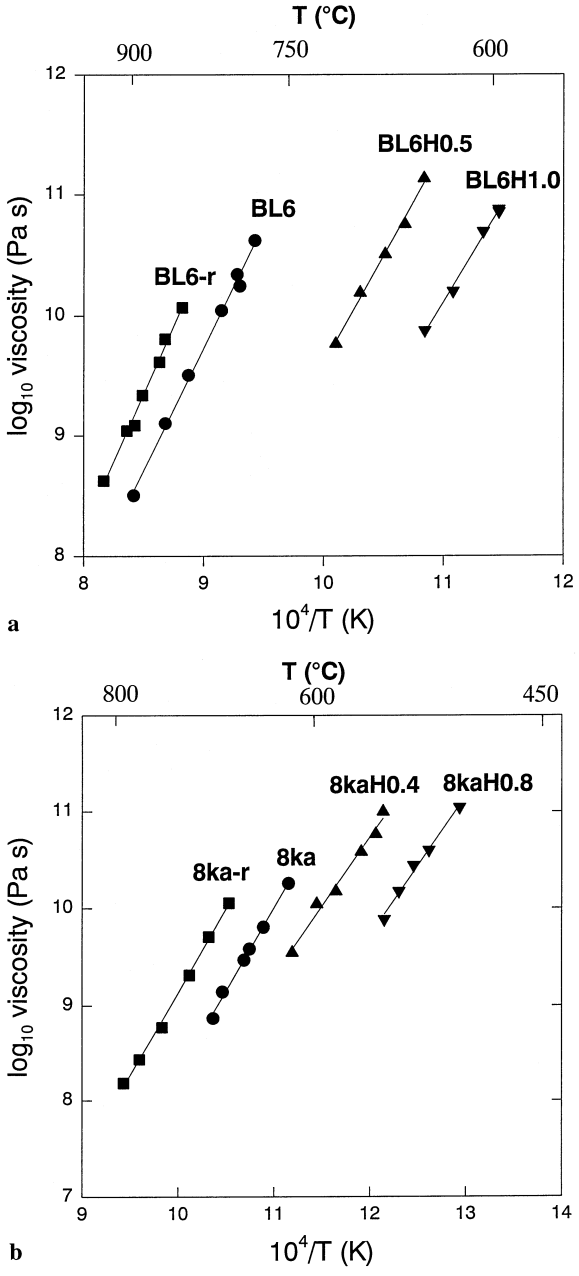

Fig. 3 Viscosity of the **a** BL6 series of samples and **b** the 8ka series

resulting in small amounts of water being lost from the sample (Table 2). Therefore, the most reliable experimental points (filled symbols in Fig. 2) are those where composition, texture, and water contents were unchanged during viscometry experiments (Stevenson et al. 1996).

Figure 3 shows the effect of water on the temperature dependence of viscosity for a calc-alkaline and peralkaline suite of samples, respectively. For the BL6 series (Fig. 3a), where the only compositional difference between samples is water content, there is a marked decrease in viscosity and a decrease in activation energies of viscous flow. The peralkaline samples (Fig. 3b) show similar activation energies for both the 8ka-r and 8ka samples. This is reflected in other peralkaline rhyolitic pairs (see Table 4). For samples containing 0.4 and 0.8 wt.% water, E_η is 17% lower than that of the reference sample 8ka-r.

Figure 4 shows log viscosity plotted at a constant temperature (1000 K) vs water content for calc-alkaline rhyolites and some peralkaline rhyolites. Linear extrapolations are less reliable for water-rich peralkaline melts (e.g., 8ka-H0.4 and H0.8) due to the likelihood of non-Arrhenian temperature dependence on viscosity as a function of the peralkalinity of the melt. Clearly, a steep variation in viscosity is seen for the addition of

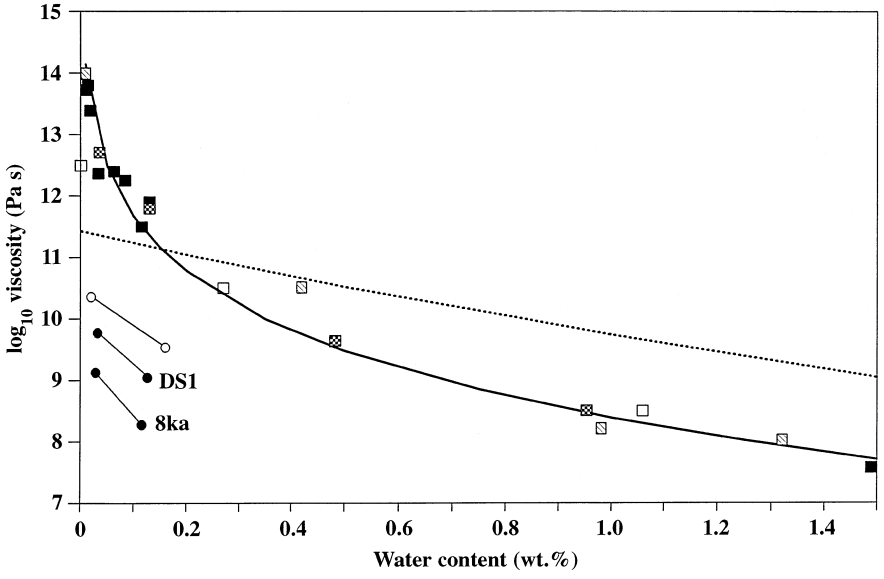

Fig. 4 Log viscosity (at 10^4/T = 10) vs water content. Peralkaline rhyolites (*filled circles*) and peraluminous macusanite (*open circles*) plot off the trend defined by calc-alkaline rhyolites (*black squares*), BL6 samples (*dark-gray squares*), HPG-8 (*light-gray squares*) from Dingwell et al. (1996), and the calc-alkaline andesite (*open squares*) from Richet et al. (1996). The Hess and Dingwell (1996) calculation scheme defined by the *solid curve* closely fits the experimental data for the calc-alkaline compostions, whereas the Shaw (1972) method (*dotted line*) poorly approximates experimental data

0.1–0.2 wt.% water. Plotted also are the data of Dingwell et al. (1996) and Richet et al. (1996) which lie on the calc-alkaline trend. Data shifted to lower viscosities include peraluminous and peralkaline compositions. The Shaw calculation scheme (for BL6) poorly approximates all experimental data and is up to two and a half orders of magnitude too low at low water contents (< 0.2 wt.%) and one and a half orders of magnitude too high for water contents in excess of 0.2 wt.%. In contrast, the Hess and Dingwell (1996) calculation scheme compares favorably with experimental data for calc-alkaline samples but overestimates viscosities for peralkaline samples. Further investigation to systematize the effect of H_2O on the viscosity of peralkaline melts are in progress (Dingwell et al. 1998).

When investigating the magnitude of ΔT at a constant viscosity or $\Delta\eta$ at a constant temperature, the former is a more reliable because, at a constant viscosity, almost all experimental data can be intersected, avoiding the need for extrapolations. This is not the case for a plot of $\Delta\eta$ vs volatile content, where extrapolations are necessary. Such extrapolations are problematic because, over larger T and η intervals, increasing water or peralkalinity yields non-Arrhenian behavior (Hess et al. 1995; Wilding et al. 1995; Richet et al. 1996; Dingwell et al 1996; Hess and Dingwell 1996). Consequently, a plot of ΔT vs volatile content is used here for conditions near Tg (at a viscosity of 10^{11} Pa s) to predict the effect of volatiles on the magnitude of the shift in T for all rhyolitic melts (Fig. 5). All remelted samples plot near the origin of this diagram. Naturally occurring obsidians from lava flows and welded fall units plot in the lower corner of the diagram, and the water-bearing Red Hills sample plots in the upper right corner. The BL6 and 8ka series (including the semi-synthetic hydrated samples) fall within the central part of a broadly linear trend as defined by all data points. The ΔT at a constant viscosity as a function of volatile content (essentially water) has also been plotted based on the calculated data from the BL6 and 8ka samples using Shaw's (1972) method; it significantly deviates from experimental data.

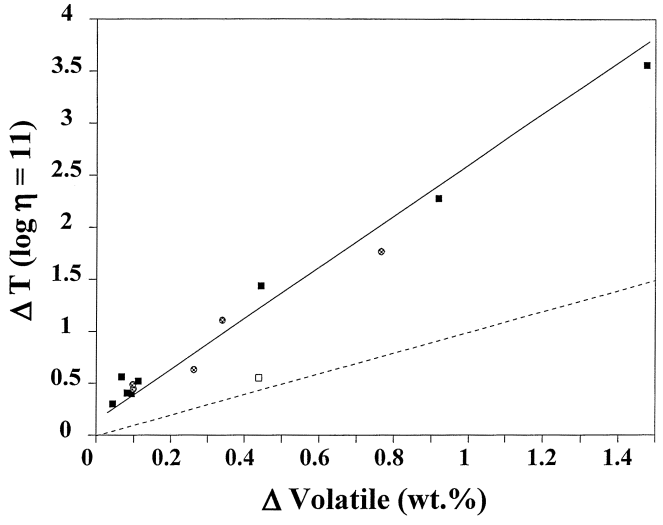

Fig. 5 The difference between the viscosity of water-bearing and remelted obsidians (ΔT) at a constant viscosity (h = 10^{11} Pa s) vs D volatiles (wt.%) for all samples: calc-alkaline rhyolites (*black squares*); peralkaline rhyolites (*circles*); and peraluminous macusanite (*open square*). Most samples define a linear trend (*solid line*) which differs markedly from ΔT from viscosity data using the Shaw scheme (*dotted line*). F-rich KE5 and MAC are shifted to the right due to loss of F when making remelted glasses

For some samples (especially KE5 and MAC) the gap in temperature–viscosity space is caused by both water and F. From less well-constrained XRF and electron probe data, the effect of changes in Cl content between annealed and natural rhyolites appears to be less significant. Indeed, most calc-alkaline rhyolites have

low Cl and F contents close to the detection limit of these analytical methods. Consequently, for these samples, the major volatile by far is H_2O. Because some F has been lost during preparation of MAC-r and KE5-r in addition to the H_2O lost, data for MAC and KE5 have been displaced off the apparent linear trend.

Conclusion

Experimental determination of the influence of traces of water on the viscosity of peralkaline and calc-alkaline natural volcanic glasses demonstrate that the calculation model of Hess and Dingwell (1996) reproduces very well the trends in viscosity and activation energy produced by the addition of water to calc-alkaline rhyolitic melts, but not those trends produced by the addition of water to peralkaline rhyolites. We therefore strongly recommend that calculation scheme for applications involving calc-alkaline rhyolites, but not for those involving peralkaline rhyolites.

Acknowledgements We thank F. Holtz for hydrations of some samples and M. Pichavant and M. Nowak for experimental guidance. This work was supported by "Deutsche Forschungsgemeinschaft" (DFG Di 431/3). Helpful reviews by P. Richet and an anonymous reviewer, as well as careful editing by M. Carroll, greatly improved the paper.

References

Bagdassarov NS, Dingwell DB (1992) A rheological investigation of vesicular rhyolite. J Volcanol Geotherm Res 50:307–322

Dingwell DB (1991) Redox viscometry of some Fe-bearing silicate melts. Am Mineral 76:1560–1562

Dingwell DB, Webb SL (1990) Relaxation in silicate melts. Eur J Mineral 2:427–449

Dingwell DB, Romano C, Hess K-U (1996) The effect of water on the viscosity of a haplogranitic melt under P-T-X conditions relevant to silicic volcanism. Contrib Mineral Petrol 124:19–28

Dingwell DB, Hess K-U, Romano C (1998) Extremely fluid behavior of hydrous peralkaline rhyolites: experimental data and model. Earth Planet Sci Lett 158:31–38

Dunbar NW, Kyle PR (1992) Volatile contents of obsidian clasts in tephra from the Taupo volcanic zone, New Zealand: implications to eruptive processes. J Volcanol Geotherm Res 49:127–145

Fontana EH (1970) A versatile parallel-plate viscometer for glass viscosity measurements to 1000 °C. Ceram Bull 49 (6): 594–597

Gent AN (1960) Theory of the parallel plate viscometer. Br J Appl Phys 11:85–88

Ghiorso MS, Sack RO (1991) Fe–Ti oxide geothermometry: thermodynamic formulation and estimation of intensive variables in silicic magmas. Contrib Mineral Petrol 108:485–510

Hess K-U, Dingwell DB (1996) Viscosities of hydrous leucogranitic melts: a non-Arrhenian model. Am Mineral 81:1297–1300

Hess K-U, Dingwell DB, Webb SL (1995) The influence of excess alkalies on the viscosity of a haplogranitic melt. Am Mineral 80:297–304

Lowenstern JB, Mahood GA (1991) New data on magmatic H_2O contents of pantellerites with implications for petrogenesis and eruptive dynamics at Pantelleria. Bull Volcanol 54:78–83

Manley CR, Fink J (1987) Internal textures of rhyolite lava flows as revealed by research drilling. Geology 15:549–552

Neuville DR, Courtial P, Dingwell DB, Richet P (1993) Thermodynamic and rheological properties of rhyolite and andesite melts. Contrib Mineral Petrol 113:572-581

Newman S, Stolper EM, Epstein S (1986) Measurements of water in rhyolitic glasses: calibration of an infrared spectroscopic technique. Am Mineral 71:1527–1541

Pichavant M, Valencia Herrera J, Boulmier S, Briqueu L, Joron L-L, Juteau M, Marin L, Michard A, Sheppard SMF, Treuil M, Vernet M (1987) The Macusani glasses, SE Peru: evidence of chemical fractionation in peraluminous magmas. Geochem Soc Spec Publ 1:357–373

Pocklington HC (1940) Rough measurement of high viscosities. Proc Cambridge Phil Soc 36:507–508

Richet P, Lejeune A-M, Holtz F, Roux J (1996) Water and the viscosity of andesite melts. Chem Geol 128:185–197

Roux J, Holtz F, Lefeure A, Schulz F (1994) A reliable high-temperature setup for internally heated pressure vessels: applications to silicate melt studies. Am Mineral 79:1145–1149

Shaw HR (1972) Viscosities of magmatic silicate liquids: an empirical method of prediction. Am J Sci 272:870–889

Stevenson RJ, Briggs RM, Hodder APW (1993) Emplacement history of a low-viscosity, fountain-fed pantelleritic lava flow. J Volcanol Geotherm Res 57:39–56

Stevenson RJ, Dingwell DB, Webb SL, Bagdassarov NS (1995) The equivalence of enthalpy and shear stress relaxation in rhyolitic obsidians and quantification of the liquid–glass transition in volcanic processes. J Volcanol Geotherm Res 68:297–306

Stevenson RJ, Bagdassarov NS, Romano R (1996) Vesiculation processes in a water-rich calc-alkaline obsidian. Earth Planet Sci Lett

Stolper EM (1982) Water in silicate glasses: an infrared spectroscopic study. Contrib Mineral Petrol 81:1–17

Taylor BE (1991) Degassing of Obsidian Dome rhyolite, Inyo volcanic chain California. Geochem Soc Spec Publ 3:339–353

Tobolsky AV, Taylor RB (1962) Viscoelastic properties of a simple organic glass. J Phys Chem 67:2439–2442

Webb SL, Dingwell DB (1990) Non-newtonian rheology of igneous melts at high stresses and strain rates: experimental results for rhyolite, andesite, basalt, and nephlenite. J Geophys Res 95:15695–15701

Westrich HR, Stockman HW, Eichelberger JC (1988) Degassing of a rhyolitic magma during ascent and emplacement. J Geophys Res 93 (B6): 6503–6511

Wilding M, Dingwell DB, Webb SL (1995) Evaluation of a relaxation geospeedometer for volcanic glass. Chem Geol 125:137–148